Design and Performance Analysis of a Digital Acoustic Telemetry System for the Short Range Underwater Channel

JOSKO CATIPOVIC, ARTHUR B. BAGGEROER, MEMBER, IEEE, KEITH VON DER HEYDT, AND DONALD KOELSCH

(Invited Paper)

Abstract—**This paper presents the design and performance description of a microprocessor based Digital Acoustic Telemetry System (DATS). The system was used to transmit data over short range underwater paths and to measure the fading characteristics of a group of CW tones. This work reports on the test results from Woods Hole Harbor. The system has also been used for under-ice propagation experiments in Lake Caanan, NH, and in the Marginal Ice Zone near Svalbard. Geometries chosen for the tests are representative of the short range marine work site paths for which high data rate communications systems are desirable.**

I. INTRODUCTION

SHALLOW WATER acoustic paths are best described as highly reverberant, fading communication channels, but complete channel descriptions are not available in the literature. A main part of this work is to determine experimentally the relevant statistics of such a path and to implement a statistically optimal communication system in this environment. The Digital Acoustic Telemetry System (DATS) was designed and built as an experimental tool for quick evaluation of transmission and coding methods and was used extensively in Woods Hole Harbor for a variety of tests ranging from very short range (~20 m) CW fading measurements to extended data transmissions at ranges up to 1 km. Most high data rate acoustic telemetry systems attempt to operate with coherent signaling since this leads to better performance. This is done by tracking the channel and careful attention to reducing multipath influences; for example, deep-ocean near-vertical-path acoustic telemetry systems operate this way [11]. Shallow water environments at high frequencies, however, are very different. They fade and have an extensive multipath structure. As the presented data show, the DATS signal fades strongly at even the very short transmission ranges. This work suggests that any realistic shallow water marine channel is fully saturated at frequencies around 50 kHz and requires an incoherent data transmission system. The channel is substantially different from the deep ocean vertical propagation path for which a number of communication systems have recently been developed, and it is unrealistic to expect that most of the systems developed for deep water will perform adequately over shallow worksite channels.

The DATS performed as expected, but it is evident that with realistic power and transmission distance constraints, increasingly complex data codes must be used to transmit information in this environment with fidelity and speed comparable to that of transmission systems operating over other channels.

II. DATS SYSTEM DESIGN

The DATS is an incoherent multiple frequency shift keying (MFSK) system. It accepts digital input, performs a selected coding operation, and modulates the coded word onto a set of sinusoids. The selected sinusoids are transmitted for a duration T, which determines the data transmission rate. (See Fig. 1.)

At the receiver, the data is quadrature demodulated and Fourier transformed using the FFT algorithm. The FFT outputs are the demodulator statistics supplied to the decoder. The coding and decoding algorithms are all implemented in software, and are easily changed. The system throughput is enhanced by software and hardware provisions for several decoder CPU's to execute in parallel, thus partially alleviating the processing bottlenecks which occur when no dedicated decoding hardware is used.

The DATS transmitter is shown in Fig. 2 [1], [2]. It consists of a digitally controlled frequency generator which can simultaneously output up to 16 tones at frequencies between 45 and 55 kHz. The tone frequencies may be changed as fast as once per millisecond by a resident 8085 CPU. In addition to the tones used for data transmission, the system continuously outputs a 60-kHz Doppler pilot tone which is used to correct for the mean Doppler drift between the transmitter and receiver. A short pulse centered at 30 kHz is output at the beginning of each data word. It is used for synchronizing the transmitter and receiver. The receiver uses the synch pulses to restart the data sampling, FFT, and decoding operations for each data word. The DATS uses a 4 × 8 element electronically steerable transmitter array with a beamwidth of 7° × 14° to reduce the channel multipath and improve the signal-to-noise ratio (SNR) [2].

The block diagram of the DATS receiver is shown in Fig. 3. The front end of the receiver is a preamplifier with 20–60 dB AGC. The signal is separated into the data band, the synchronization pulse, and the Doppler pilot tone by bandpass

Manuscript received September 10, 1984; revised October 2, 1984.

J. Catipovic is with the M.I.T.-WHOI Joint Program, Cambridge, MA 02139.

A. B. Baggeroer is with the Department of Ocean Engineering, Massachusetts Institute of Technology, Cambridge, MA 02139.

K. von der Heydt and D. Koelsch are with Woods Hole Oceanographic Institution, Woods Hole, MA 02543.

0369-9059/84/1000-0242$01.00

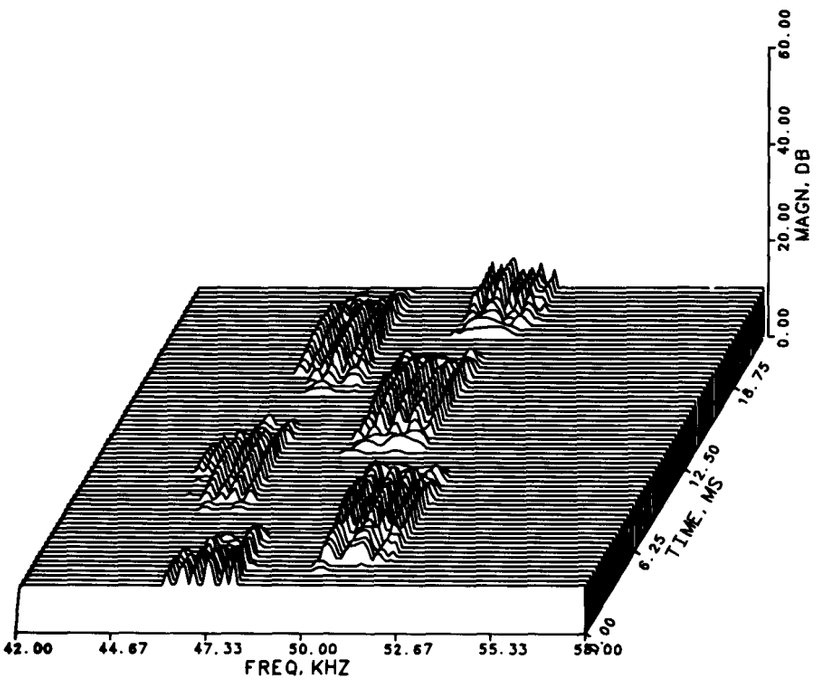

Fig. 1. Modulator frequency hopping.

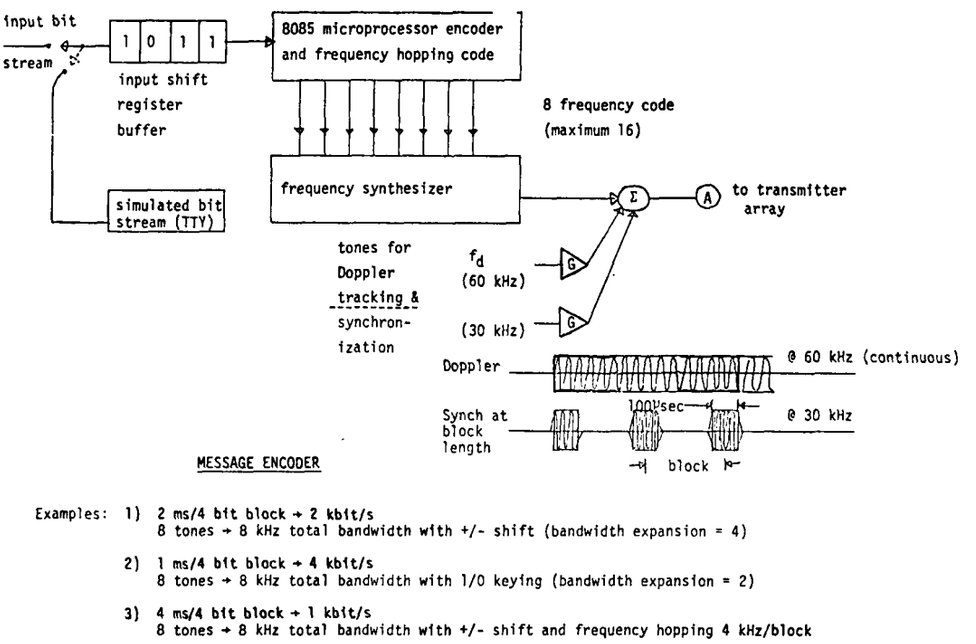

Examples: 1) 2 ms/4 bit block → 2 kbit/s
8 tones → 8 kHz total bandwidth with +/- shift (bandwidth expansion = 4)

2) 1 ms/4 bit block → 4 kbit/s
8 tones → 8 kHz total bandwidth with 1/0 keying (bandwidth expansion = 2)

3) 4 ms/4 bit block → 1 kbit/s
8 tones → 8 kHz total bandwidth with +/- shift and frequency hopping 4 kHz/block

Fig. 2. DATS encoding and modulation system.

filtering. The data channel is demodulated by a 50-kHz carrier derived from the Doppler pilot tone, and each signal quadrature is filtered to 5 kHz by a 36 dB/octave low-pass filter. The synchronization pulse, centered at 30 kHz, is bandpass filtered and then threshold detected. A delay-locked loop tracks the frame duration and supplies an internally generated frame pulse in the event of an input dropout.

The Doppler pilot tone is separated through a high $Q(Q = 200)$ ceramic filter. The received tone is used to generate the 50-kHz data demodulating frequency. It is tracked coherently by a CMOS single-chip phase-locked loop (PLL) which performs acceptably until amplitude fluctuations become severe. In that case, a 50-kHz demodulating tone is synthesized internally by the receiver, and one has to give up Doppler shift corrections. The PLL output is digitally multiplied by 5 and then divided by 6 to obtain the 50-kHz nominal

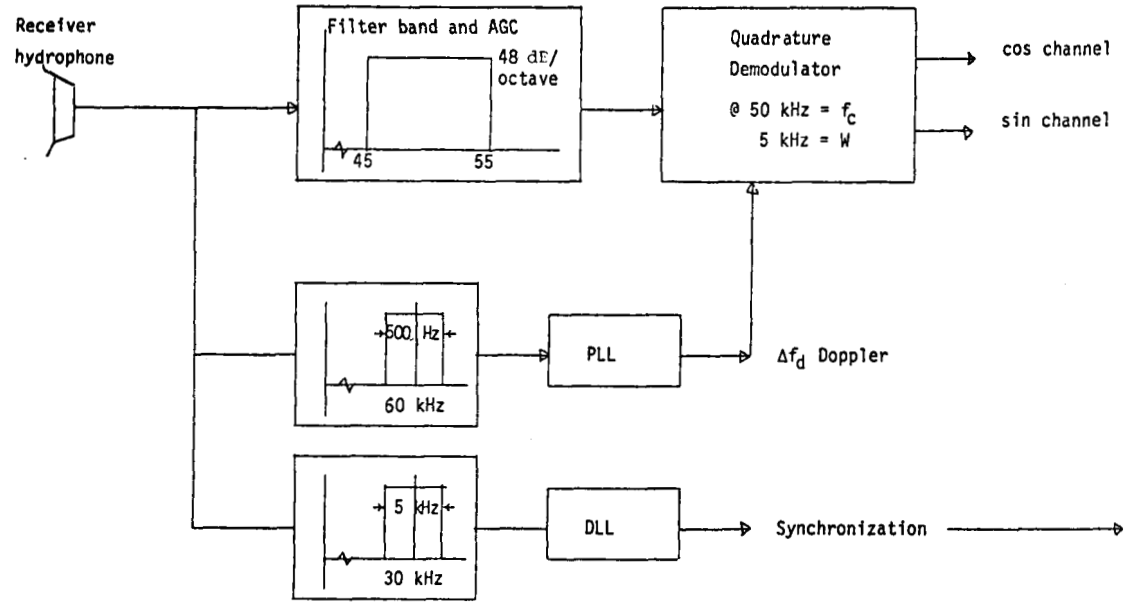

Fig. 3. DATS receiver block diagram.

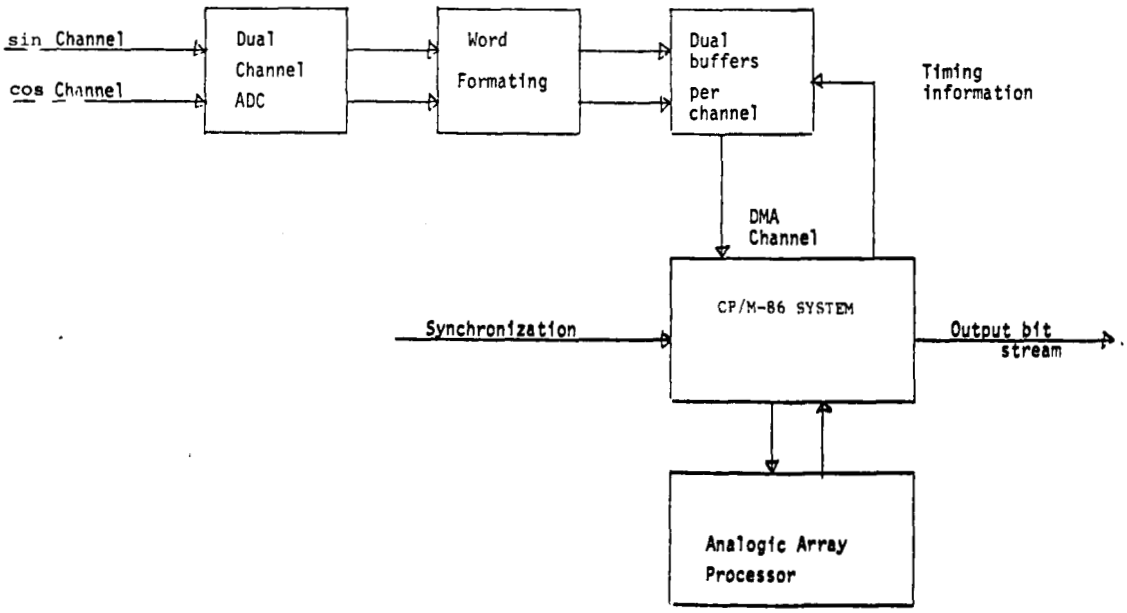

Fig. 4. DATS demodulator hardware.

demodulating frequency, whose quadratures are multiplied by the received data signal. The Doppler bandwidth of the system is 600 Hz. As 1 kn ($\sim$0.5 m/s) of relative motion between the receiver and transmitter produces 17.5 Hz of Doppler shift at 50 kHz, the system is capable of correcting up to an 16-kn relative velocity.

The diagram of the data demodulator is shown in Fig. 4. It consists of a bank of filters matched to all possible transmitted tones followed by squarers and decoders for each possible code word. After the initial signal conditioning, all the receiver operations are done digitally. Both quadratures of the demodulated data are sampled simultaneously and then converted into two 8-bit integers which are DMA-transferred to the processor. The matched filters are implemented with an FFT on an array processor, and the decoding is done by an 8086-based microprocessor system.

The DATS receiver software operating environment, while using CP/M-86 as the base operating system, is designed to allow several concurrent processors to execute parts of the decoding program independently in real time. A manager program executing on a master CPU can allocate decoding tasks to different slave processors. This parallel processing allows the decoding of moderately complex codes without constraining the system throughput rate. Furthermore, the DATS allows for easy and inexpensive modifications of the coding algorithms. Such codes can be evaluated and compared

in real time over actual in-water propagation paths, and the pertinent decoder parameters processed and/or saved for either *in situ* or later analysis.

The DATS is designed for incoherent data transmissions over a fading channel. Such a channel may be considered as composed of many signal scatterers, each of which contributes a delayed and Doppler shifted signal replica to the received waveform. When the number of scatterers is large, it is convenient to consider the average of scattered energy received after a certain delay and Doppler shift. Such information is expressed in terms of the channel scattering function, which depicts the average received signal strength versus time delay and Doppler shift [5], [9]. Other quantities of interest closely related to the channel scattering function are the 2-frequency correlation function $F(\Delta w, t)$, and the narrowband envelope time correlation function $R(t_0, t)$ [3], [5], [7]. They are related by the following transforms of the channel scattering function $b(\tau, f)$:

$$R(t_0, t) = \int\int b(\tau, f) \exp [j2\pi f(t_0 - t_1)] \, d\tau df \quad (1)$$

$$F(\Delta w, t) = \int\int b(\tau, f) \exp [j\Delta w\tau + 2\pi ft] \, d\tau df. \quad (2)$$

The scattering function is a more complete channel description than either $F(\ )$ or $R(\ )$, but its measurement in the DATS environment requires very high resolution processing. For use in system design, we found direct measurements of $F(\ )$ and $R(\ )$ more expeditious, particularly since the system configuration is based on rough estimates of the two functions and is insensitive to their detailed structure [5].

The first moments of $F(\Delta w, t)$ in frequency and $R(t_0, t)$ in time represent the mean shift of received energy in the frequency and time domains. The second moments are the ms spread around the mean. They are important parameters in the design and performance of the DATS. The total RMS frequency spread B influences the total received tone bandwidth. If the bandwidth of the transmitted tone is W, the received bandwidth is $W + B$, so the minimum tone spacing must be set at $W + B$. If the mean Doppler shift is not compensated, B represents the total Doppler drift and spread. The DATS receiver effectively removes the mean Doppler drift. B then represents only the RMS scatter around the mean Doppler shift, and is consequently much smaller, allowing the system to improve bandwidth use.

The RMS time spread of the received waveform T influences the temporal correlations of the received waveforms. If T is comparable to or larger than the duration L, intersymbol interference results since each word becomes contaminated by delayed echoes of the previous transmissions. To reduce the effects of time spreading, the modulator is capable of frequency hopping. This operation is illustrated in Fig. 1. For this example, the tone frequencies are separated by increments of 250 Hz, and the modulator hops to a new set of frequencies for transmitting each word. The hopping partially clears the channel of multipath and reduces the degree of saturation and intersymbol interference at the expense of additional decoder errors while tracking the hop band sequence and bandwidth consumption.

The initial code implemented on the DATS relies on signal bandwidth and frequency hopping to overcome the effects of fading. It is an (8, 4) Hamming code where each 4-bit data word is coded into 8 bits with the following coding matrix:

$$\begin{bmatrix} 1 & 0 & 0 & 0 \\ 0 & 1 & 0 & 0 \\ 0 & 0 & 1 & 0 \\ 0 & 0 & 0 & 1 \\ 0 & 1 & 1 & 1 \\ 1 & 0 & 1 & 1 \\ 1 & 1 & 0 & 1 \\ 1 & 1 & 1 & 0 \end{bmatrix} = H. \quad (3)$$

where $y = Hx$, y = code word, and x = data. The receiver tracks the frequency hopping pattern of the transmitter and matches the squared outputs of the input FFT with the previously stored tone patterns. The decoder implements a soft-decoding algorithm, where the squared magnitudes of the FFT outputs for the eight tones comprising each word are added, and the word corresponding to the largest sum declared the output. The flowchart of the algorithm to decode the (8, 4) Hamming code is shown in Fig. 5. Note that the decoder operations are pipelined so that four or five frames of data may either be processed simultaneously by different processors, or sequentially if only one 8086 CPU is used. A number of data storage, processing, and display routines are available, and operate asynchronously with the framing pulse. They are prioritized, so if there is insufficient time to process all of them, lower priority routines are automatically deleted until there is time to process them again. During normal system operation the display routines often lag the decoder by more than 20 frames, because the time required to track hop bands and store experiment outputs varies with signal-to-noise ratios, error probability, and the channel reverberation level.

The decoder is fast enough to keep up at rates of up to 2 kbit/s with the simple block code used. The data transfer speed was limited by the frame duration required for an acceptable signal-to-noise ratio and the time to accumulate enough data samples for the required decoder FFT resolution. For example, a word frame 2 ms long yields a data rate of 2 kbit/s with the (8, 4) code used. At a typical complex digitizing rate of 16 kHz, the receiver operates on 32 complex data points, and the FFT output consists of 32 independent samples with a total bandwidth of 8 kHz, i.e., a sample every 500 Hz.

While the bandwidth used by the code is considerably less than the available decoder bandwidth, frequency hopping was used to spread out the transmitted energy over the entire band. This creates an even more stringent rate/performance tradeoff since a faster code requires more bandwidth for each tone, and less is available for frequency hopping. The bandwidth limitations are thus based on the channel time spread L, and the tone bandwidth W. Strictly, one should add the channel frequency dispersion B to the bandwidth required for each tone, but we found B to be negligible compared to the individual tone bandwidth W in all experiments.

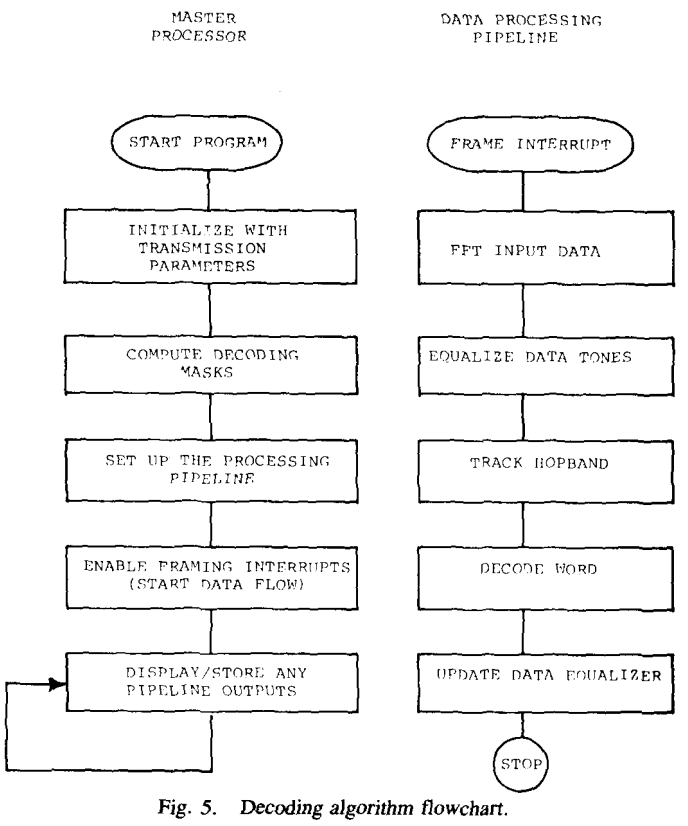

Fig. 5. Decoding algorithm flowchart.

A more significant constraint on the tone spacing is the channel coherence bandwidth. Figs. 12 and 13 show that for the two experiments conducted, there exists an independently fading path every 2 kHz. The bit bands available on the DATS are generally considerably narrower than this. One gains no advantages by spacing signals closer than approximately 2 kHz other than increasing the signal power present in a single fading path. The DATS generally has available from 5 to 10 dB of SNR for realistic operating distances. A well-known result [5] requires approximately 5 dB for each independently fading path; thus the number of independent paths should be maximized, that is, the individual tone bandwidth should be increased as high as possible given the above constraints.

III. TRANSMISSION CHANNEL MODEL AND MEASUREMENTS

A. Modeling Channel Behavior

This section presents measurements of the underwater acoustic channel used at frequencies centered at 50 kHz and at ranges of up to 1 km in shallow water. An attempt is made to measure parameters relevant to digital data communication and classify the channel based on these measurements.

Consider a communications channel where the received signal is a sum of many scattered replicas of the transmitted waveform. If several scatterers are substantially stronger than the rest and their amplitude and phase are at least partially known, it is customary to treat their contribution to the received field as a specular component and separate it in the analysis from the field due to the rest of the scatterers. A common example of this case occurs when the direct, i.e., nonscattered path constitutes a significant part of the received field. Alternatively, one may consider several dominant scatterers as making up the specular path.

The channel behavior of interest in the design of DATS is the random modulation of a tone. A commonly used model for the fading bahavior of a CW carrier uses the Rician probability density function to describe the instantaneous carrier amplitude. Since the quantity of interest to the DATS decoder is the square of a narrow-band tone envelope, this work uses instead the noncentral χ^2 density to model the behavior of the square of the tone envelope. The DATS is an MFSK system, and the soft decoding algorithm sums the squares of M received signal envelopes. Such a sum may be modeled by a noncentral χ^2 density with $2M$ degrees of freedom.

Consider a channel composed of a large number of scatterers. Then if

$$s(t) = e^{jw_1 t} \tag{4}$$

is transmitted, the received signal may be modeled as [5]

$$r(t) = \sum_{i=1} A_i e^{j[w_1 t + \theta_i]}$$

$$= be^{j[w_1 t + \theta]} \tag{5}$$

where

$$be^{j\theta} = \sum_{i=1} A_i e^{j\theta_i}. \tag{6}$$

The received signal may be divided into the specular and random component

$$be^{j\theta} = a_1 e^{j\phi_1} + a_2 e^{j\phi_2} \tag{7}$$

where the a_1 and ϕ_1 are deterministic (although possibly unknown) and a_2 is random, distributed as $N(\theta, V_2)$, and ϕ_2 is random and uniformly distributed. Then the density of b is Rician (assuming θ unknown and uniformly distributed):

$$P_b(b) = \frac{b}{V_2{}^2} \exp\left[\frac{a_1{}^2 + b^2}{2V_2}\right] I_0\left[\frac{a_1 b}{V_2{}^2}\right]. \tag{8}$$

Now we consider the processing of the received signal. The optimal receiver for a channel with a specular propagation component implements the following equation:

$$l = \frac{V_2{}^2}{N_0} |b|^2 + a_2 \text{ Re } [be^{-j\theta}]. \tag{9}$$

The DATS receiver does not track the coherent signal component for ease of implementation and because low specular signal levels were expected. As shown below, the specular signal level was found to be low for all but the very short ranges. The DATS demodulator thus performs the following operation on each data frame to get the statistic $B(nT)$, as illustrated in Fig. 6

$$B(nT) = \left|\frac{2}{T}\int_0^T r(t) \sin (w_1 t)\, dt\right|^2 + \left|\frac{1}{T}\int_0^T r(t) \cos (w_1 t)\, dt\right|^2. \tag{10}$$

The performance loss due to this receiver implementation decreases as the channel becomes more saturated. Even when

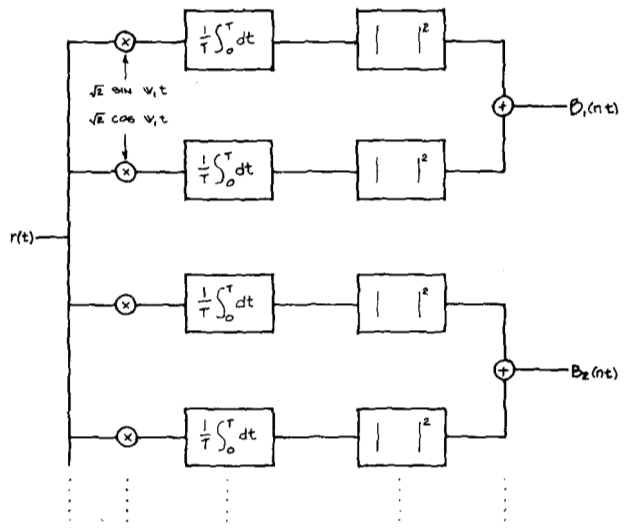

Fig. 6. DATS demodulator processing schematic.

the specular strength is twice that of the scattered component, the performance degradation may be considered negligible [8]. To evaluate the receiver performance, we approximate the averaging integral:

$$B(nT) = \left| \frac{1}{T} \int_0^T be^{j[wt+\theta]} \sin (w_1 t)\ dt \right|^2 + \left| \frac{2}{T} \int_0^T be^{j[wt+\theta]} \cos (w_1 t)\ dt \right|^2. \quad (11)$$

The expression is difficult to deal with unless b is assumed constant during each integration. We conveniently assume that the bandwidth of b is much less then $1/T$, the reciprocal of the integration time, and hence b may be taken outside the integral. For the data presented, this assumes the bandwidth of b to be much less than 100 Hz. Then:

$$B(nT) = \left| b(nT)e^{j\theta} \frac{1}{T} \int_0^T \sin^2 (w_1 t)\ dt \right|^2 + \left| b(nT)e^{j\theta} \frac{1}{T} \int_0^T \cos^2 (w_1 t)\ dt \right|^2 \quad (12)$$

where $b(nT)$ is the averaged envelope of the nth data block and has the same probability density function as $b(t)$. Squaring and summing the two quadratures gives:

$$B(nT) = b^2(nT). \quad (13)$$

The density of $B(nt)$ may be written as

$$P_B(B) = \frac{1}{\sigma^2} \exp \left[\frac{-(B+a_1^2)}{2\sigma^2} \right] I_0 \left[\frac{\sqrt{B}a_1}{\sigma^2} \right] \quad (14)$$

$$P_B(B) = \frac{1}{\sqrt{\pi\sigma^2}} \exp \left[\frac{-(B+a_1^2)}{2\sigma^2} \right] \sum_{i=0}^{\infty} \frac{(a_1^2)^i B^i}{(\sigma^4)^i} \frac{\Gamma(i+\frac{1}{2})}{\Gamma(i+1)} \quad (15)$$

$$\sigma^2 = V_2^2 + N_0^2$$

which is the noncentral χ^2 distribution with two degrees of freedom and the noncentrality parameter equal to the square of the specular component a_1.

The DATS next adds M $B(nT)$'s (corresponding to M different tone frequencies) to produce a statistic corresponding to the total received energy for a particular code word. This yields a noncentral χ^2 density if the individual $B(nT)$'s are independent and their variances are equal. It is reasonable to assume that the ratio of specular to scattered energy is the same for all tones, and that the additive noise is white. Then the equal variance assumption is valid. On the other hand, there is usually some correlation between envelope fading at different frequencies, and, in general, the envelope amplitudes may not be considered independent without examination of the carrier frequency separation and the channel behavior.

B. Experimental Results

To estimate the correlation functions for modeling channel behavior and the resulting DATS performance, a number of CW experiments were carried out. The measurements were collected in Woods Hole Harbor, MA, with the DATS system. The transmitter broadcast a "chord" of eight equally-spaced unmodulated tones. The tone spacing was fixed at 1000 Hz. The received and amplified data were quadrature demodulated, digitized, blocked, and fed to an array processor which performed 128-point complex FFT computations. The squared magnitude of the FFT was saved for further processing. Each data frame length was fixed at 10 ms for envelope measurements. The processing was performed in real time on the continuously-sampled input, so no time gaps appear in the data. Typically 3–5 min of data were processed during each experiment, and the results were saved on a floppy disk. The output consists of sixteen FFT output points from each frame. These include the eight points at the broadcast frequencies, and interspersed between those, eight data points representing the additive noise energy halfway between the broadcast tones. A time series of this data collected over a 20-m shallow water path is shown in Fig. 7. This plot represents the encountered fading behavior for most propagation paths, as detailed fading characteristics are difficult to distinguish from short records when presented in this format. Note that the log of the squared magnitude of data amplitude is plotted. It is seen that even at this short range, considerable fading is occurring. Also note the considerable frequency dependence of the received energy. The eight tones have equal energy before transmitting. The spectral shading is due to the nonideal transfer functions of the transmitting array, receiving hydrophone, and the demodulating and filtering electronics. Attempts to compensate for the system shading and measure the channel transfer function were unsuccessful because the transmitter array gain was frequency dependent along any direction but broadside, and transmitter pointing errors resulted in several decibels differences in signal magnitude across the frequency range of interest.

Histogram estimates of the probability density functions of the log of the 16 FFT outputs are shown in Fig. 8. Four thousand data points are processed for each channel. The plots

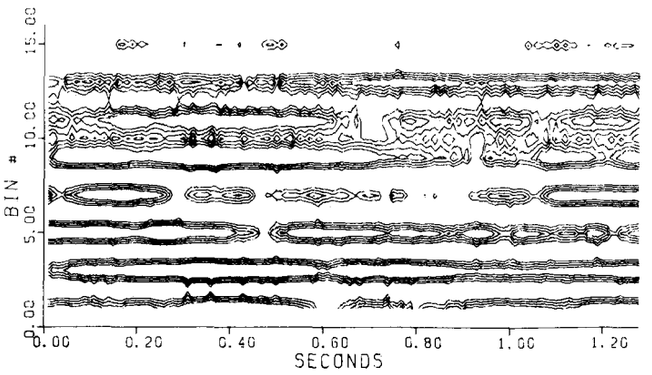

Fig. 7. Example of tone fading behavior.

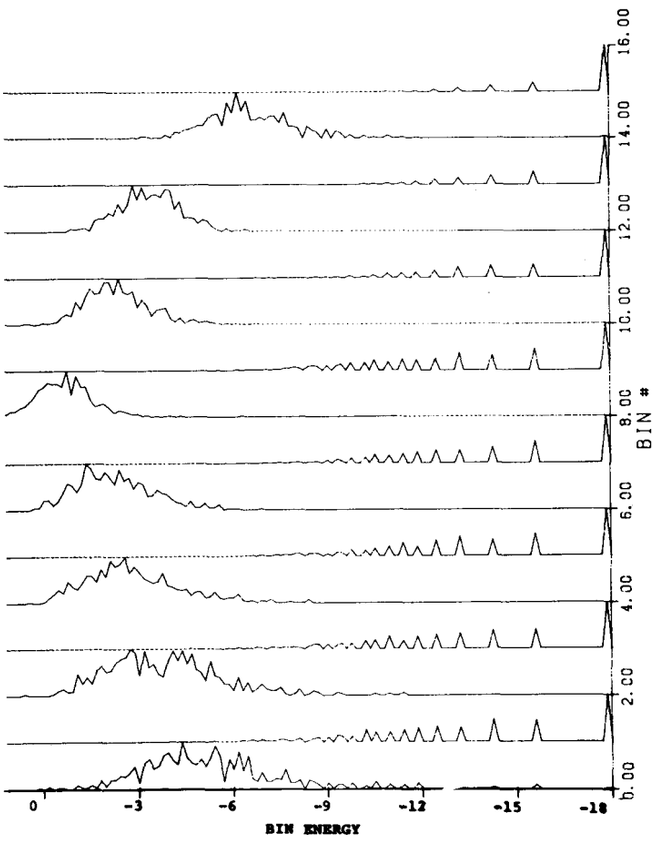

Fig. 8. PDF histograms—short path.

are normalized by the mode of each histogram to ease plot formating, and the vertical scales for the 16 tones may thus be different. The abcissa range is the same for all 16 functions, so that the relative energy distributions in the 16 channels may be directly compared. The data in this format represents the density function of the squared signal envelope.

Fig. 9 shows results of an identical experiment for an approximately 800-m-long path across Woods Hole Harbor. The propagation path was in water approximately 6–18 m deep, with the transmitter fixed approximately 2 m off the bottom in 9 m of water and the receiver close to the surface. During the experiment the sea surface, agitated by a 20-kn ($\sim$10 m/s) wind, was generally foamy with a considerable number of breaking waves. Since the harbor is sheltered, the waves were seldom higher than 0.3 m.

As expected, the relative strength of the specular path decreased with increased source–receiver separation, but not as drastically as might be anticipated from the 20-m results. The longer-range experiment was done with more open surroundings, and excited fewer secondary paths, but the primary path was also more attenuated, i.e., both the direct and the reverberant fields were lower for the second experiment (the noncentral x^2 model (15) is applicable in each case).

Figs. 10 and 11 show the time correlation functions of the

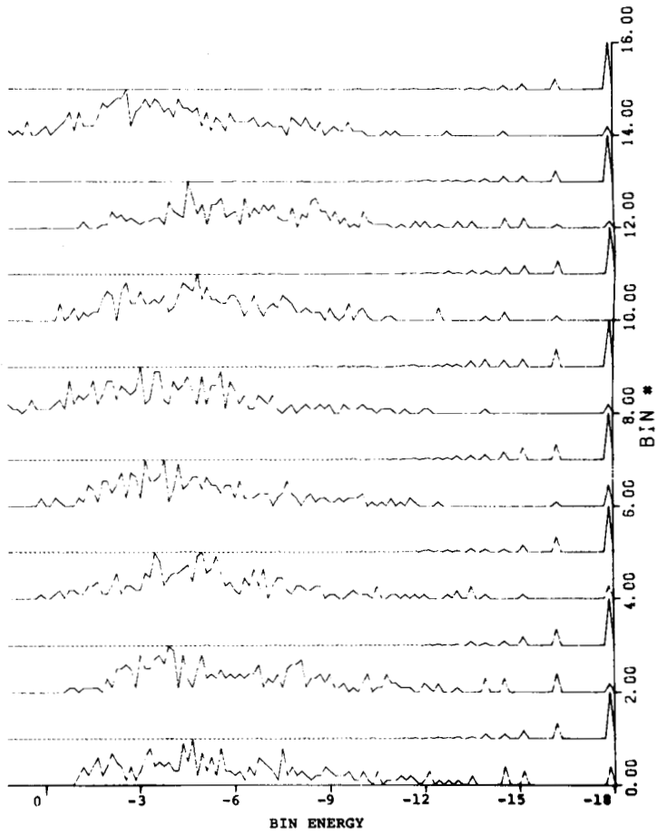

Fig. 9. PDF histograms—long path.

16 FFT outputs. Five hundred data points per channel were used to estimate the first 250 lags of the autocorrelation functions. The time series was assumed to be stationary. The eight noise channels show no time correlation. As seen in Figs. 8 and 9, their envelopes appear Rayleigh, and it is reasonable to conclude that the noise is well modeled by the white Gaussian assumption. The data channels exhibit a characteristic correlation time of several tenths of a second, indicating an RMS Doppler spread B of several hertz, and it is seen that the longer-range signals fluctuate more slowly. Expected fade duration is several tenths of a second. The longer features (approximately 1 s) of the envelope correlations are believed due to the fluctuations of the specular path. In particular, the motions of nearby berthed ships were noted to be correlated with the tone amplitudes.

Since a data transmission error for a coded MFSK system requires a simultaneous dropout of several data channels, the frequency correlation of the tone fading is of interest. This data is useful for determining the number of diversity paths in the channel [5]. Figs. 12 and 13 show the frequency correlations of the eight data tones. Five hundred data points per channel were used to compute the eight correlation lags for the eight data channels. Both plots indicate significant frequency correlation of the data tones, separated by 2–3 kHz, and suggest that a single diversity path occupies several kilohertz. The channel time spread L is thus 1/2–1/3 ms.

IV. DATA TRANSMISSION RESULTS

Together with the CW transmissions, each harbor experiment included a 6-h data transmission. The data transmission rate was 400 bit/s. Twelve-hundred bit-per-second experiments were also carried out, but the reduced bit SNR at the higher data rate caused higher error rates and error logging problems. A pseudorandum word sequence was used, so the receiver could compare the received word stream with a stored replica of the transmission to identify transmission errors. It also computed the bit SNR by dividing the energy levels of the eight detected tones by the energy levels in the eight unused frequency bins. The SNR was averaged for 256 data frames, then stored on disk together with the number of transmission errors during the same period.

Before the in-water transmission experiments, the additive white Gaussian noise (AWGN) channel was simulated in the laboratory by summing the transmitted signal with the output of an analog white noise generator. This served as a system calibration run and a benchmark for fading channel performance tests. The noise power was varied to span a range of SNR conditions, and the test was conducted for a total of 12 h. The SNR and error logging procedures were the same as during the water tests and synchronization errors were avoided by directly connecting the transmitter and receiver. It was found that again the synchronization system performed substantially worse than the data decoder at low SNR. However, DATS is

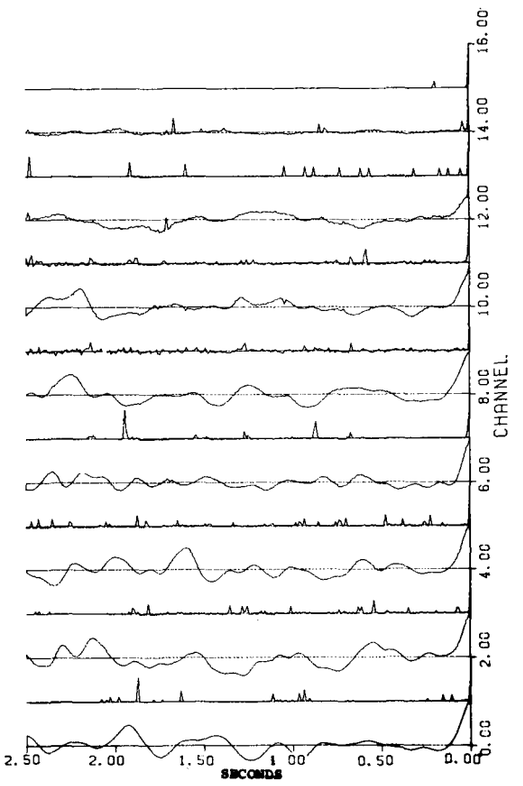

Fig. 10. Time correlation—short path.

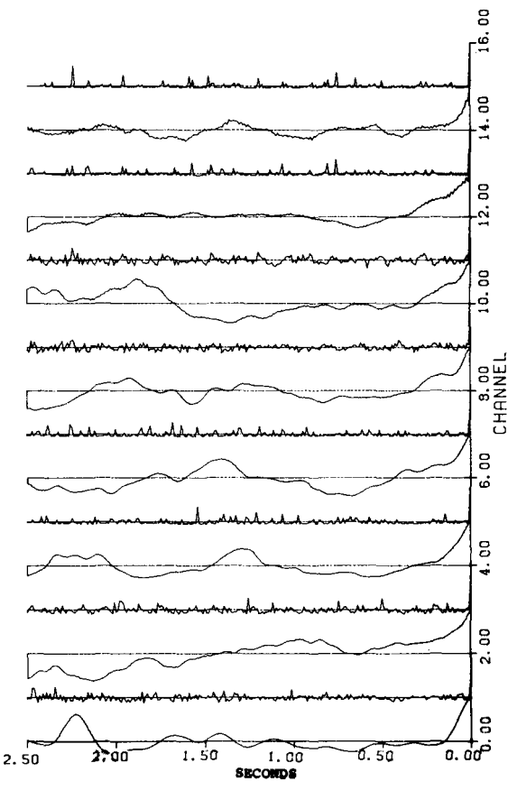

Fig. 11. Time correlation—long path.

not designed to operate over the AWGN channel, and the data is presented because the AWGN is a benchmark and to illustrate the relative performance levels achieved over the two channels.

The in-water data errors consisted of transmission errors, and timing synchronization errors due to errors in tracking the beginning of each data chord. The synch system performed acceptably as long as deep signal fades were infrequent. The two types of errors were detected and tallied separately. Any presented data reflects only the transmission errors, which at times represented but a small part of the overall error rate. The problems with the synch system result from the fading of the pulses. The receiver is implemented with a delay-lock loop which is able to track the pulses across a short ($\sim$100-ms) dropout. If the fade is substantially longer, the receiver begins to search for the pulses, and does not lock again for up to several seconds. As the data transmission during the synch search is garbled, a very large increase in overall error probability results. The system is probably inadequate for a strongly fading channel.

To illustrate the difference between the fading and the AWGN channel, Fig. 14 shows the predicted and observed DATS performance over the Rayleigh channel, and Fig. 15 shows the same information over an AWGN channel. Both the uncoded and the (8, 4) Hamming coded expected system behavior is shown. On the AWGN channel, both conditional densities are still χ^2 as in the fading case, but the noncentral parameter of the true hypothesis depends on SNR, and the performance improves more quickly with SNR.

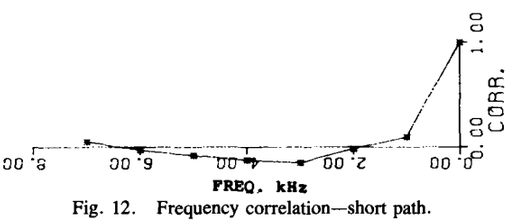

Fig. 12. Frequency correlation—short path.

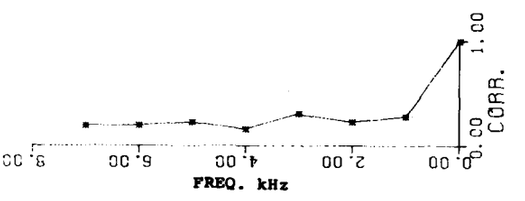

Fig. 13. Frequency correlation—long path.

The receiver performance may be modeled by considering it as a hypothesis test between the tone groups. Consider first a hypothesis test with one tone; the generalization to n tones follows directly. If H_1 is true, there is a fading tone at f_1, and white noise plus leftover reverberant energy at f_2, and if H_2 is correct, there is a tone at f_2 and noise at f_1. The receiver computes the square of the averaged complex envelope in each of the two frequency bins. Then the hypothesis test consists of distinguishing between two χ^2 random variables. If the channel allows a specular propagation path, one of the

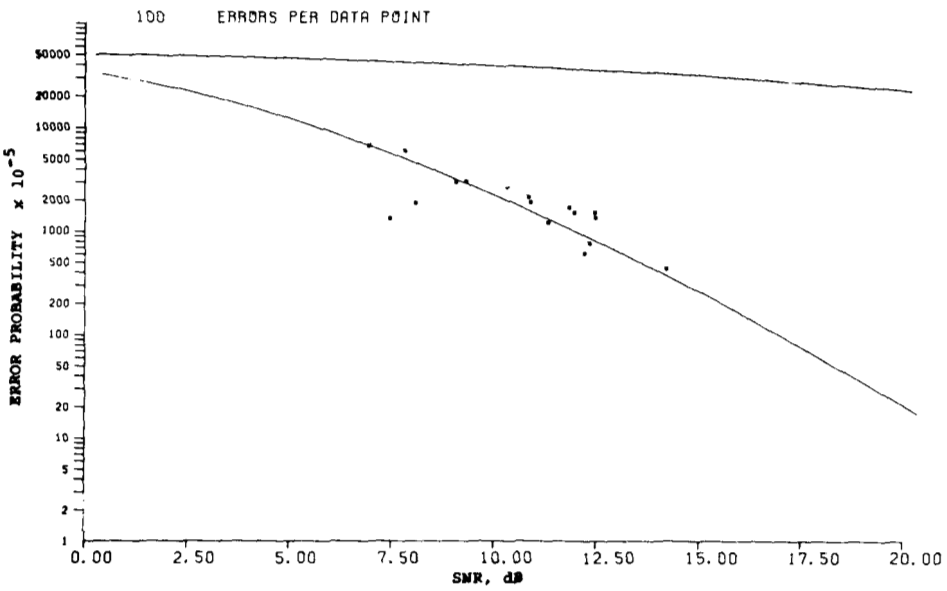

Fig. 14. DATS performance—Rayleigh channel.

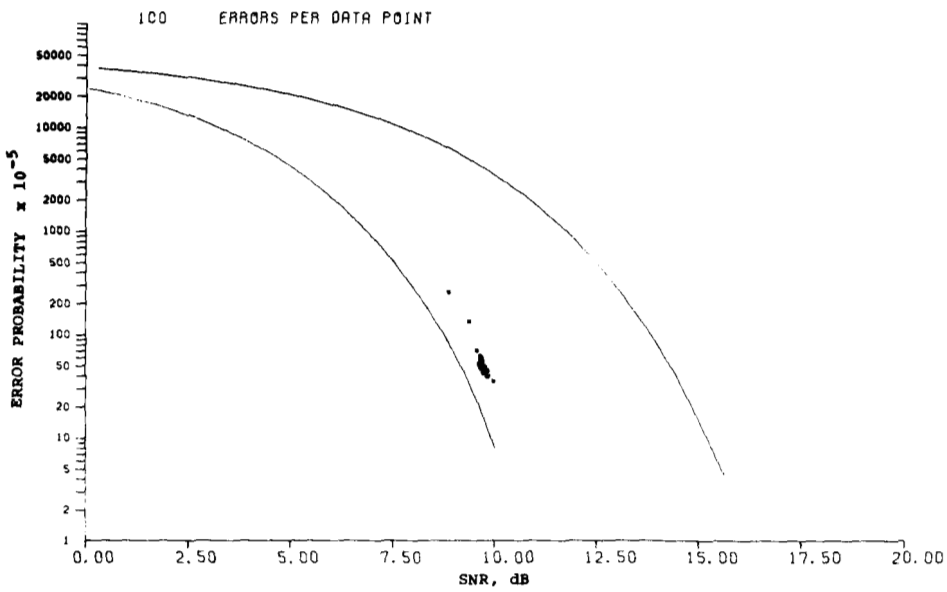

Fig. 15. DATS performance—AWGN channel.

variables has a noncentral χ^2 distribution. The probability of error for this hypothesis test is given by Turin [8] for both the coherent and incoherent receiver. The probability of error for an incoherent receiver is given by

$$\text{Pr. error} = \frac{1}{2}\frac{N_0}{(V_2^2 B(nT) + N_0)} \cdot \exp\left[-\frac{B(nT)a_1^2}{2(V_2^2 B(nT) + N_0)}\right] \tag{16}$$

Now consider a test with four tones present under each hypothesis, relevant because the code distance is 4. In other words, the two words differ by four tones, so to decide between them the receiver compares the sums of 4 tone energies. The test consists of comparing the sum of squares of the four tone envelopes, namely:

$$\sum_{i=1}^{4} B_i(nT) \overset{?}{\gtrless} \sum_{j=1}^{4} B_j(nT). \tag{17}$$

One may assume that the B^1s are independent variables, or equivalently, that the different tones fade independently. In the communication channel encountered, this would be justified if the tone separation is greater than 2 kHz, and the assumption would provide an upper performance bound if the tone separation is narrower. Then the sums are χ^2 random variables with 8 degrees of freedom. The variable corresponding to the true hypothesis has a noncentral distribution.

If there is no intersymbol interference in the time domain, i.e., if there is no "leftover" specular energy from a previous transmission, the other variable is χ^2 with 8 degrees of

freedom. Intersymbol interference may be modeled in two ways. Correlated fading reduces the number of degrees of freedom of the statistic, and reverberation increases the energy level of the "false" hypotheses. Both of these effects tend to overlap the two conditional densities more, and thus increase error probability. Temporally correlated fading would make the error probabilities of successive words dependent, and thus control the "burstiness" of the errors. It would not influence the error probability of a single word.

In all cases the system performance is somewhat worse than predicted. A substantial part of the degradation is due to the spectral shaping of the transmitted signal by both the transmitting and the receiving equipment, as is evident in Figs. 8 and 9. Equalizing the transmitted waveform is difficult because of the frequency hopping and other rapid frequency variations of the transmitted waveform. The transmitter hydrophones, in particular, have a peaked transfer function. The time synchronization pulse, at 30 kHz, and the Doppler pilot tone, at 60 kHz, are also attenuated severely, but the amplitudes are compensated before transmission.

At the receiver the signal is further shaped by the receiving hydrophone and the front end electronics. This spectral shaping is easily corrected by the digital demodulator, which attempts to whiten the input spectrum, and may be neglected if the equalizer is performing properly. Equalizing a waveform shaped before transmission, however, introduces SNR variation from path to path and thus colors the additive noise. Thus the decoding consists of choosing between sums of Gaussian variables whose means and variances differ. Computing error performance then becomes substantially more difficult, and seems universally avoided in the literature. The uniform path case serves as an upper performance bound.

One-kilohertz tone separation, as used in the above experiments, is not sufficient to guarantee an independent fading path for each tone. Thus the test statistics have fewer degrees of freedom than considered in the performance prediction, and this, too, is expected to degrade observed performance.

The most significant problem inherent in the high-frequency acoustic communication channel is the paucity of independent propagation paths. A single path for several kilohertz of carrier frequency in an environment already bandwidth-constrained by attenuation makes for a situation worse than that expected when the system was designed.

There have been several attempts at coherent communication which used either the nonfading deep ocean path or concentrated on baffling and system beam patterns for the reduction of secondary returns. The results and data rates attained are superior to those described here, but DATS is designed to operate under more adverse conditions, particularly those encountered around marine worksites which are typically noisy and cluttered with strong scatterers. Although the DATS performance reasonably reflected the theoretical predictions, both the ultimate achieved performance and the level of "tweaking" and system maintenance required to achieve the described performance indicate that increasingly sophisticated coding and a mechanically simpler system need to be employed for future underwater communications systems.

REFERENCES

[1] A. B. Baggeroer, D. Koelsch, K. von der Heydt, and J. Catipovic, "DATS—A digital acoustic telemetry system for underwater communications," in *Oceans '81 Conf. Rev.* (Boston, MA), Sept. 1981, pp. 55–60.

[2] W. Hanot, "A phased array sonar for an underwater acoustic communications system," M.S.O.E. thesis, M.I.T., Cambridge, MA, Aug. 1980.

[3] P. Bello, "Characterization of randomly time-variant linear channels," *IEEE Trans. Commun. Syst.*, vol. CS-11, pp. 360–393, Dec. 1963.

[4] S. Flatte, Ed., *Sound Transmission Through a Fluctuating Ocean.* New York: Cambridge Univ. Press, 1979.

[5] R. Kennedy, *Fading Dispersive Communication Channels.* New York: Wiley-Interscience, 1969.

[6] P. Mikhalevsky, "Envelope statistics of partially saturated processes," *J. Amer. Statist. Assoc.*, pp. 151–158, July 1982.

[7] W. L. Root, "On the measurement and use of time-varying communication channels," *Inform. Contr.*, vol. 8, pp. 390–422, 1965.

[8] G. L. Turin, "Error probabilities for binary symmetric ideal reception through nonselective slow fading and noise," *Proc. IRE,* vol. 46, pp. 1603–1691, 1958.

[9] H. L. Van Trees, *Detection, Estimation and Modulation Theory.* New York: Wiley, 1968.

[10] A. Viterbi, *Principles of Partially Coherent Communications.* New York: McGraw-Hill, 1966.

[11] G. R. Mackelburg, S. J. Watson, and A. Gordon, "Benthic 4800 bits/second acoustic telemetry," in *Oceans '81 Conf. Proc. Rev.* (Boston, MA), Sept. 1981, p. 72.

[12] J. F. Pieper, J. G. Proakis, R. R. Reed, and J. K. Wolf, "Design of efficient coding and modulation for a Rayleigh fading channel," *IEEE Trans. Inform. Theory*, vol. 24, pp. 457–468, July 1978.

★

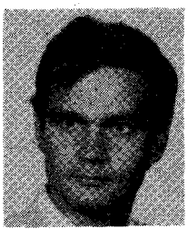

Josko Catipovic was born in Zagreb, Yugoslavia, on March 29, 1959. He received the B.S. degree in electrical engineering and the B.S. degree in ocean engineering from the Massachusetts Institute of Technology, Cambridge, MA, in 1981.

He is currently a Research Assistant in the Massachusetts Institute of Technology–Woods Hole Oceanographic Institution Joint Program in Oceanographic Engineering. His research interests include high-frequency acoustic channel modeling and acoustic telemetry.

★

Arthur B. Baggeroer, for photograph and biography, see this issue, p. 235.

★

Keith von der Heydt was born in 1949. He received the E.S.E.E. degree from Lehigh University, Bethlehem, PA, in 1971.

On the technical staff at Woods Hole Oceanographic Institution, Woods Hole, MA, since 1976, he is a member of the Ocean Engineering department. For the past 6 years, he has been heavily involved with Arctic acoustics, focusing on hardware and software development for the acquisition of data from low-frequency hydrophone arrays.

★

Donald Koelsch, photograph and biography not available at time of publication.